Lidar Backscatter from Horizontal Ice Crystal Plates

C. M. R. PLATT[1]

Cooperative Institute for Research in Environmental Sciences, University of Colorado/NOAA, Boulder, Colo. 80309

(Manuscript received 7 November 1977, in final form 4 January 1978)

ABSTRACT

Some unusual lidar returns from an altostratus cloud are interpreted in terms of reflections from hexagonal ice plates falling with their long axes aligned in the horizontal. Such an explanation is consistent with the observed high backscatter coefficients and low depolarization ratios and also with the temperature range (−12 to −20°C) of the cloud layers, as well as the known fall characteristics of naturally occurring ice platelets. Backscatter efficiencies are calculated for "perfect" ice platelets when illuminated at or near an axis orthogonal to the crystal long axis. It is shown that very high backscatter coefficients can potentially be measured from a cloud of ice plates, depending on the fraction of crystals which are "perfect," the degree to which the plates' long axes stay horizontal, and the angle of the lidar to the vertical.

It is further shown that reflection from a single crystal gives an appreciable signal-to-noise ratio at the receiver and that only a few crystals will be correctly aligned in the horizontal in a typical laser pulse volume, and for realistic particle number densities.

1. Introduction

Lidar observations made on an altostratus cloud on 9 August 1975 revealed a layered structure possessing variable optical properties (Platt, 1977). The topmost layer was characterized by very high backscatter coefficients and an apparent large backscatter to extinction ratio. At the same time, the measured depolarization ratio was generally in the range from 0.03 to 0.05, except near the bottom of the layer. Because of these characteristics, the cloud layer was interpreted as composed of small droplets; however, it was pointed out then that an alternative explanation could be that the strong backscatter and low depolarization could occur from horizontally oriented hexagonal ice plates. If such an explanation were true, then the backscatter characteristics would give a means of identifying the cloud as an ice cloud in a certain phase of development, and could be used for such identification. Previous work (Schotland *et al.*, 1971; Sassen, 1974; Derr *et al.*, 1976) has revealed quite a wide range of depolarization ratios from ice clouds, with a characteristic value of about 0.4 for hexagonal ice columns and bullets, and high values, often greater than unity, from virga at the base of storm clouds. It thus seems that depolarization measurements on mixed phase clouds may give information not only on the particle phase (Sassen, 1974), but also on the *type* of ice crystal and its evolution. The suggestion that ice plates can give a unique lidar signature is explored further in this note.

2. Growth and fall characteristics of hexagonal ice plates

The temperature range from −8 to −25°C is one in which ice crystals grow as hexagonal plates. In the range from −12 to −15°C where the greatest growth rate occurs, dendritic plate crystals may also form (Mason, 1968), although these require a water-saturated environment. Initially, a plate grows in three dimensions, until its short axis is about 50 μm. At this point, the long axis is about 1200 μm and any further growth occurs mainly along this axis (Ono, 1969). When the crystal obtains sufficient fall velocity, the ventilation around the crystal will favor water supersaturation near the edges of the plates, which will cause dendritic growth. According to Ono, the rate of dendritic growth accelerates rapidly as the crystal diameter increases from 200 to 400 μm. If plate crystals are present in a cloud of mixed phase, then attachment of small frozen drops (riming) will occur when the crystal diameter is greater than about 400 μm. In Ono's measurements in natural clouds, the size distribution of plates had a rather sharp peak in the 200–400 μm diameter region. Crystals with diameters less than 100 μm and greater than 400 μm were rare.

The fallspeed of plates increases with increasing diameter, but for diameters >100 μm, the fall velocity is independent of diameter and is about 35 cm s^{-1} (Fletcher, 1962). Jayaweera and Mason (1965) studied the behavior of freely falling discs and columns in a viscous fluid. For Reynolds numbers ($\mathrm{Re}=vd/\nu$, where v is fall velocity, d crystal diameter and ν kinetic viscosity) less than 0.01 (very small crystals), the discs

[1] On leave from CSIRO, Division of Atmospheric Physics, Aspendale, Australia.

0021-8952/78/0482-0488$05.00

had no preferred orientation. For $0.01 \quad Re < 0.1$ the discs oriented themselves to offer maximum resistance to motion, i.e., the long axis horizontal. They remained oriented and fell with a steady motion until $Re \geqslant 50$. At this point, a persistent fluttering occurred. At a temperature of $-20°C$ and pressure of ~ 330 mb, Re varies between 0.07 for a 10 μm diameter crystal to 14 for a 2000 μm crystal. Thus most plate crystals in the atmosphere should fall with their long axes horizontal. Strong evidence for this fall characteristic of plates in the real atmosphere is provided by Ono's observations of the riming pattern of plate crystals (Ono, 1969). For dendrites, however, some oscillation or flutter apparently occurred.

3. Backscatter characteristics of ice plates

Generally, the crystal dimension for the long axis is much greater than the laser wavelength (0.69 μm for ruby laser). In that case, light is backscattered either as a specular reflection from the front and back surfaces of the crystal or as a skew reflection and refraction involving the front, side and back surfaces. If a plate is falling with its long axis horizontal, it will cause only a specular reflection to a vertically pointing lidar. If the lidar is pointing *away* from the vertical, only skew rays backscattered through internal reflections will be observed.

Consider a parallel-sided plate illuminated as illustrated in Fig. 1. As ice is nearly transparent at visible wavelengths, then light will be reflected from the front and back surfaces in nearly equal amounts. As the reflectance of ice is small, contributions from further internal reflections will be negligible. Suppose that an amplitude of light a is reflected from each crystal surface. If the surfaces are plane parallel and the ice is homogeneous, then interference between the beams from the two surfaces can occur. Thus the reflected amplitude will be $2a\cos(\delta/2)$ where $\delta = 2\pi t \sec\theta/\lambda$ and t is the crystal thickness, θ the angle of incidence and λ the wavelength. The normal reflected intensity I will be

$$I = 4a^2 \cos^2\delta/2. \tag{1}$$

Thus the reflected intensity will go through maxima and zero as t or θ change.

It is not clear from past work as to whether ice crystal plates in the atmosphere have sufficiently plane parallel surfaces or are sufficiently homogeneous to give interference effects. The work of Sassen (1977) indicates that interference probably does not occur. In that case the reflected intensities would add incoherently from the two surfaces to give a total intensity of $2a^2$. In the analysis that follows, this latter case is assumed.

The volume sampled by a lidar pulse typically contains many thousands of cloud particles. However, in a natural cloud, it can be anticipated that horizontal-falling ice plates will possess some degree of "flutter"

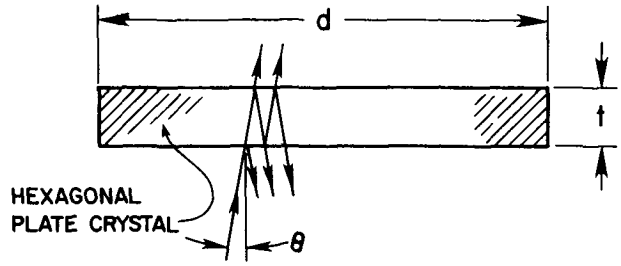

FIG. 1. Multiple reflections from a plate crystal.

about the horizontal, caused by small-scale turbulence, larger scale eddies, wind shear, or riming and dendritic growth (Jayaweera and Mason, 1966). In this case, only those crystals correctly oriented in the horizontal will give specular reflection to a lidar receiver, and it is not obvious that there will be many such crystals. However, we consider first the hypothetical case where the transmitter pulse volume does contain sufficient correctly aligned crystals to enable us to define an average backscatter efficiency per crystal, and to average out interference effects if they are indeed occurring. We shall subsequently calculate the probable number of correctly aligned crystals in a typical lidar pulse volume and the signal from each such crystal.

The lidar backscatter intensity at the receiver will depend on the number of crystals in the pulse volume, the crystal diameters, and the angles of departure of the crystal long axes from the horizontal. For an ensemble of crystals which are taking up every possible angle between the horizontal and some maximum angle of displacement $\delta\xi$, only those crystals which are normal to the incident laser beam will reflect radiation specularly back to the receiver. More accurately, those crystals displaced through an angle $< \delta\psi$ from the horizontal will reflect back to the receiver, where $\delta\psi$ is half the angle subtended by the receiver aperture. Now, as $\delta\xi$ increases, the probability of a crystal being favorably oriented diminishes. Without an exact knowledge of the motion of the crystal long axes as they "flutter" about a horizontal plane, the probability of favorable orientation cannot be predicted accurately. However, if the angles of flutter are very small, the crystals would not experience any great rotational accelerations, so that to a good approximation it can be argued that all angles of the crystal long axis between horizontal and maximum angle of flutter are equally likely. Further, it is assumed that the planes of rotation of the crystals are randomly oriented in the horizontal.

Now the angle through which the long axis rotates during one complete flutter is $2\delta\xi$, so that radiation is reflected away from the vertical within an angle of $4\delta\xi$. If the solid angle around the angle $4\delta\xi$ is $\delta\Omega$, then for a large ensemble of crystals within the transmitter pulse volume the average backscatter cross section J_b per unit steradian is given by

$$J_b = 2RA/\delta\Omega, \tag{2}$$

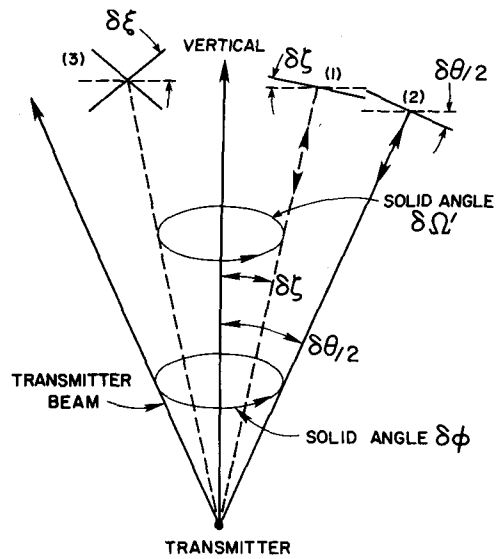

FIG. 2. Schematic of transmitter beam. Crystal (1): maximum angle of flutter $\delta\xi=\delta\zeta$, $\delta\zeta<\delta\theta/2$; reflection to receiver only within cone, solid angle $\delta\Omega'$. Crystal (2): maximum angle of flutter $\delta\xi=\frac{1}{2}\delta\theta$; reflection to receiver anywhere in cone $\delta\phi$. Crystal (3): maximum angle of flutter $\delta\xi>\frac{1}{2}\delta\theta$; reflection to receiver anywhere in cone.

where A is the cross-section area of the crystal presented to the lidar radiation and R the normal reflectance of the crystal surfaces. As it is assumed that radiation is reflected incoherently from the back and front surfaces, the total reflection is $2R$. The refractive index of ice at about 0.7 μm is 1.31 so that R is 0.02.

Referring to Fig. 2 we distinguish between two cases, depending on whether the angle of flutter $\delta\xi$ is greater or less than $\delta\theta/2$, where $\delta\theta$ is the angle defining the transmitter beam. First, let $\delta\xi\leqslant\delta\theta/2$. We assume that the lidar transmitter and receiver axes are coaxial and aligned together exactly in the vertical. (Typically, $\delta\theta$ is from 0.5 to 2 mrad and the receiver angle $\delta\psi$ is set larger than $\delta\theta$.) Only those crystals in the transmitter beam which lie within a cone of angle $\delta\xi$ ($=\delta\zeta$, say) to the vertical will be capable of reflection to the receiver. We therefore define an *effective* cross section

$$J_b(e)=[2RA/\delta\Omega][\delta\Omega'/\delta\phi],$$

where $\delta\Omega'$ is the solid angle containing the angle $\delta\zeta$, and $\delta\phi$ the solid angle of the transmitter beam. Now as $\delta\xi=\delta\zeta$, then $\delta\Omega'=\pi\delta\xi^2$ (for small angle $\delta\xi$). But $\delta\Omega=4\pi\delta\xi^2=4\delta\Omega'$ so that

$$J_b(e)=2RA/4\delta\phi. \tag{3}$$

Also since $\delta\phi=\pi\delta\theta^2/4$ ($\delta\theta\ll1$),

$$J_b(e)=2RA/\pi\delta\theta^2. \tag{4}$$

The backscatter efficiency $q(\pi)$ can be defined as the backscatter cross section per steradian divided by the geometrical cross section. Thus

$$q(\pi)=2R/\pi\delta\theta^2[\mathrm{sr}^{-1}]. \tag{5}$$

The extinction efficiency q_e is defined in a similar manner. The extinction cross section J_e of the crystals is composed of $2RA$ for reflection (entirely in the back direction) and $\sim A$ for diffraction, so that $J_e=A(1+2R)$ and $q_e=1+2R$. The backscatter-to-extinction ratio k is then defined as $4\pi q(\pi)/q_e$, so that

$$k=8R/\delta\theta^2(1+2R). \tag{6}$$

The values of $q(\pi)$ and k are seen to be independent of the angle of flutter $\delta\xi$.

The second case occurs if $\delta\xi>\delta\theta/2$. As the solid angle $\delta\Omega$ in Eq. (2) is equal to $4\pi\delta\xi^2$, then

$$k=2R/\delta\xi^2(1+2R). \tag{7}$$

To summarize, if the flutter $\delta\xi$ is less than $\delta\theta/2$, then k is constant, but if $\delta\xi$ becomes greater than $\delta\theta/2$, k decreases as $\delta\xi^2$. This dependence on $\delta\xi$ is shown in Fig. 3. which shows that k is very large for small $\delta\xi$. For comparison, the value of k is 0.65 for a model water cloud (Deirmendjian, 1964) and about 0.3 for a cirrus ice cloud (Platt, 1973). Clearly, the backscatter enhancement from near-horizontally aligned plates is potentially very large.

The above treatment predicts the average backscatter characteristics for a large number of randomly oriented crystals. It is obviously important to determine how many of such crystals are favorably aligned for reflection to the receiver in a typical transmitter volume and in a cloud containing a realistic number of plate crystals. The number will depend on the transmitter beam angle $\delta\theta$ and the depth of cloud l which is illuminated. The illuminated volume V is given by

$$V=\pi z^2\delta\theta^2 l/4, \tag{8}$$

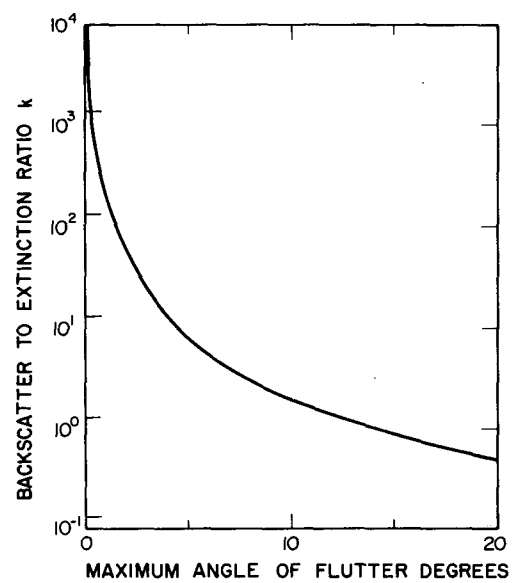

FIG. 3. Dependence of average backscatter to extinction ratio k per crystal on angle of flutter $\delta\xi$ for a laser pulse volume containing many aligned crystals.

where z is the range (altitude). When $\delta\xi < \delta\theta/2$ then the probability $P(\delta\xi)$ of correct alignment is given by

$$P(\delta\xi) = D^2/4z^2\delta\theta^2, \tag{9}$$

where D is the receiver diameter. The number of aligned crystals n_a in the volume V is thus given by

$$n_a = n_0 V P(\delta\xi) = \pi n_0 l D^2/16, \tag{10}$$

where n_0 is the number of crystals per unit volume.

If $\delta\xi > \delta\theta/2$, then

$$n_a = n_0 l D^2(\delta\theta/8\delta\xi)^2. \tag{11}$$

The number of ice crystals in clouds in the temperature range from -12 to -20°C ranges from about 1 to 100 l^{-1} (Mossop, 1968; Heymsfield, 1977). The predicted number n_a of aligned crystals from Eq. (11) is shown in Table 1 for different values of $\delta\xi$ and $n_0 = 10\,l^{-1}$, $D = 0.3$ m, $l = 3$ m (pulse length of 20 ns), $\delta\theta = 0.002$ rad. The factor f gives the proportion of crystals in the cloud which have "perfect" surfaces (see Section 5). It is apparent that for any angle of flutter greater than about 1°, the probable number of crystals which are aligned correctly becomes less than unity.

Thus, for cases of low number density and where only small height increments in a cloud are being examined, the former treatment of obtaining an average backscatter efficiency may not be valid. Even for a homogeneous cloud, the backscatter could fluctuate considerably from one pulse volume to the next. It is thus pertinent to ask whether the reflection from a single "perfect" crystal in the pulse volume would give sufficient photons at the receiver to be detected with a good signal-to-noise ratio.

If P_0 is the laser power, then the power P_i incident on a crystal of area A at range z is given by

$$P_i = P_0 A/z^2\delta\phi, \tag{12}$$

where $\delta\phi$ is the solid angle of the transmitter beam. As the angle subtended by a crystal surface at a given range from the transmitter is much less than the angle subtended by the receiver aperture at the same range, all the radiation which is reflected back by a favorably aligned planar crystal will enter the receiver. Thus the power P_R returned at the receiver will be simply equal to $2RP_i$ or

$$P_R = 0.04 P_0 A/z^2\delta\phi, \tag{13}$$

where the reflectance at the crystal is $2R$.

The number of photons n_R returned within the pulse time τ is

$$n_R = GP_R\tau, \tag{14}$$

where G is the ratio of photon number n_R to energy at the lidar wavelength. The number of electron pulses counted at the output of the receiver photomultiplier is

$$n_i = q\epsilon n_R, \tag{15}$$

where q is the photomultiplier quantum efficiency and ϵ the optical efficiency.

Fig. 4 shows n_i for different ranges and crystal diameters. Clearly, the signal recorded from a single crystal is quite large. The signal to noise ratio for each pulse is equal to $n_i^{\frac{1}{2}}$. The signal from a cloud of some depth, containing many lidar pulse lengths, will thus tend to fluctuate with range, the individual crystal pulses being dependent on the crystal size. If the interference effect given by (1) does occur it introduces an additional variable into the single crystal reflection amplitude.

TABLE 1. Number of crystals n_a oriented to give a reflection at the lidar receiver. Lidar pulse length = 20 ns, $\delta\xi$ = angle of flutter, f = fraction of "perfect" crystals.

$\delta\xi$ (deg)	f = 0.2	0.4	0.6	0.8	1.0
0.1	34.81	69.61	104.42	139.23	174.04
0.5	1.39	2.78	4.18	5.57	6.96
1	0.35	0.70	1.04	1.39	1.74
2	0.087	0.17	0.26	0.35	0.43
4	0.022	0.044	0.065	0.087	0.11
6	0.0097	0.019	0.029	0.039	0.048
8	0.0054	0.011	0.016	0.022	0.072
10	0.0035	0.0070	0.010	0.014	0.017

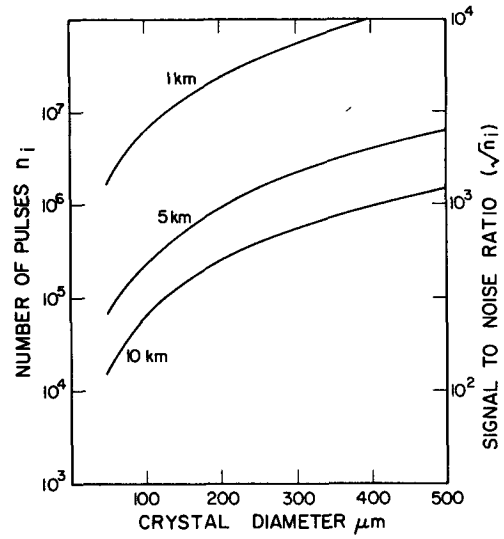

FIG. 4. Number of photons received from a single crystal reflection for various ranges versus crystal diameter.

4. Depolarization characteristics of ice plates

Liou and Lahore (1974) have studied theoretically the depolarization from hexagonal platelets. For normal reflection on the surface parallel to the long axis, the depolarization is predicted to be zero. As radiation returns to the receiver only *via* a normal reflection, the depolarization ratio for horizontal, or near horizontal,

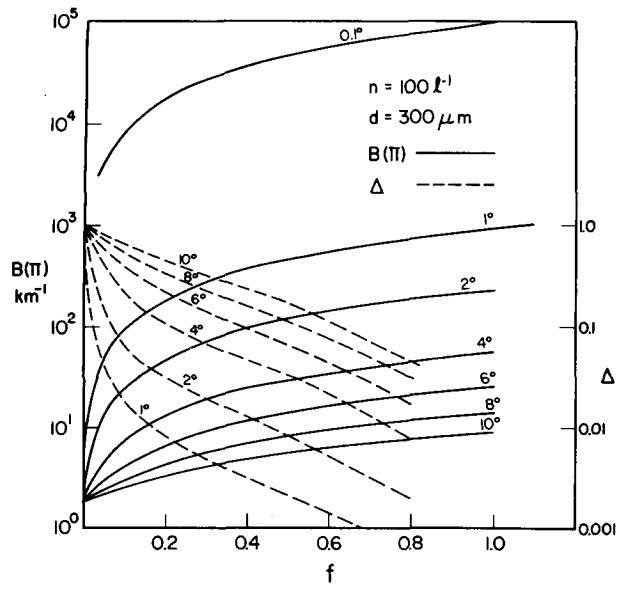

FIG. 5. Dependence of $B(\pi)_{\parallel}$ and Δ on angle of flutter $\delta\xi$ and factor f (see text).

platelets will be zero. Only if fluttering causes large departures of the crystal surfaces from the horizontal will reflections from skew rays start to give appreciable depolarization (and backscatter).

5. Model of lidar backscatter from natural clouds containing ice plates

Even if optimum conditions exist for hexagonal plate growth, there is unlikely to be a complete population of perfect plates in a natural cloud. Dendritic growth, riming and shattering can cause the scattering in the back direction to be partly non-specular. Thus lidar backscatter will be determined by both the quality of the crystals and their orientations. On the other hand, for small departures from the horizontal, the depolarization will be affected by the crystal quality only.

To illustrate these effects, we consider a simple model. This assumes that 1) a fraction $(1-f)$ of the crystals are "imperfect," i.e., they exhibit isotropic scattering and a depolarization ratio of unity (the value of k in each polarization is then 0.25); and 2) a fraction f of the crystals have perfect crystal faces, giving a depolarization ratio of zero. The crystals are assumed to have a circular cross section of diameter d. We consider the case when $B(\pi)_{\parallel}$ is integrated sufficiently in height to smooth any fluctuations to give a mean $B(\pi)_{\parallel}$. The backscatter coefficients for the two polarizations are then given by

$$B(\pi)_{\parallel}=(n_0 q_e \pi d^2/4)[2fR/\delta\xi^2(1+2R) +0.25(1-f)], \quad (16)$$

$$B(\pi)_{\perp}=(n_0 q_e \pi d^2/4)[0.25(1-f)], \quad (17)$$

where q_e is the extinction efficiency $(=1.04\approx 1)$. Also,

$$\Delta=B(\pi)_{\perp}/(B\pi)_{\parallel}. \quad (18)$$

The dependence of $B(\pi)_{\parallel}$ and Δ on f and $\delta\xi$ for one value of n_0 and d is shown in Fig. 5. As f increases, more crystals are available for reflection and $B(\pi)_{\parallel}$ increases. At the same time, the depolarized component decreases. The model forces the depolarization ratio to zero when $f=1$, which may not be exactly correct for real hexagonal crystals. It implies that Δ will be extremely small if $\delta\xi\approx 0.1°$, even if f is small. At the other extreme, Δ is forced to unity when $f=0$. Again, this may not be correct in clouds of "imperfect" crystals, where Δ may be less than unity, as in the case for cirrus clouds. However, the model does illustrate that Δ could rapidly become small with the appearance of horizontal plate crystals, even if they comprise only a small fraction of the total crystal population. The model also gives a "sensible" value of $B(\pi)_{\parallel}$ (~ 2 km^{-1}) for the case when $f=0$, although of course $B(\pi)_{\parallel}$ is dependent on both n_0 and the crystal diameter.

6. Comparison with observations

Several laboratory studies have been made which are relevant to the present topic. In these studies, depolarization in backscattering from ice crystals formed in a cold chamber was measured with continuous He–Ne lasers. Schotland *et al.* (1971) observed intensity spikes in the amplitude of the backscatter, which repeated over short periods of time. These spikes were observed mainly in the parallel polarization return; the spikes were interpreted as being specular reflections from the faces of the crystals and, qualitatively, they exhibited low depolarization. A further investigation by Sassen (1974) confirmed these results and he established that most backscatter from platelets was due to specular reflections from the crystal surfaces, and depolarization in the spike events was no more than a few percent. Liou and Lahore performed a similar experiment. Although spiking events were not so obvious, they were observing crystals in the horizontal plane, so that spiking would be mainly absent for horizontally aligned crystals.

A vertical lidar return from the altostratus cloud observed by Platt (1977) is shown in Fig. 6. The value of depolarization ratio Δ from 4.2 to 4.6 km altitude was ~ 0.4, which is the figure often observed in cirrus clouds of columnar crystals. The maximum observed backscatter coefficient of 1 km^{-1} is also rather typical of cirrus. Above 4.6 km, there is an increase of about a factor of 5–10 in backscatter coefficient, whereas the depolarization ratio falls gradually to about 0.04. The backscatter figures are affected by attenuation of the laser pulse by the lower ice layer, predicted to be at least 0.5 (Platt, 1977). Thus the maximum values of $B(\pi)_{\parallel}$ are at least 12 km^{-1} and the integrated backscatter is about 6 which is much higher than the typical

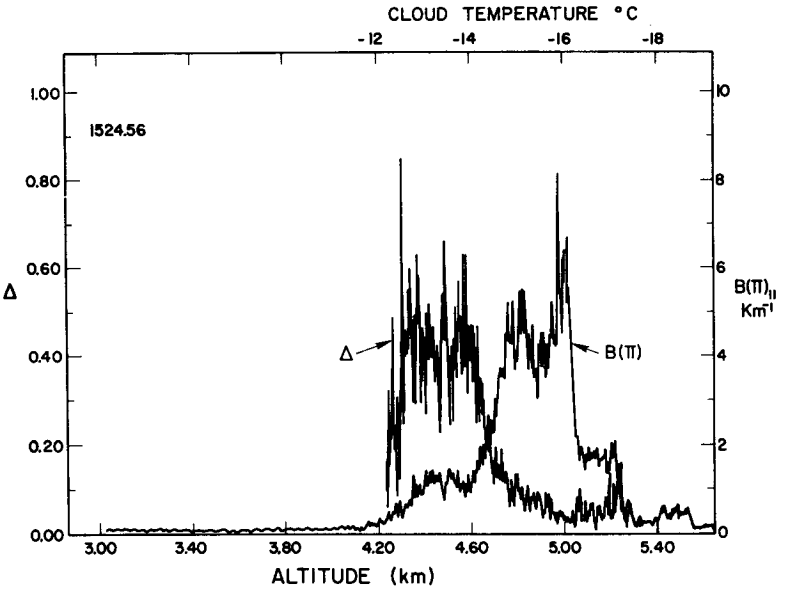

FIG. 6. Profile of $B(\pi)_{\parallel}$ and Δ obtained from an altostratus cloud with a vertical pointing calibrated lidar on 9 August 1975 (Platt, 1977).

value of ~ 0.4 measured in cirrus. The above characteristics are consistent with the backscatter from this layer being caused, at least partially, by reflections from ice crystal plates. The air temperatures in the layer are also optimum for growth of ice plates. The behavior of $B(\pi)_{\parallel}$ and Δ at the bottom of the layer is consistent, at least qualitatively, with the decrease of available plate surfaces and a growth of irregular crystals. From Fig. 5, a change in Δ from 0.04 to 0.4 corresponds, for $\delta\xi = 2$ for instance, to a change in $B(\pi)_{\parallel}$ from 40 to about 6 km^{-1}. By postulating that the crystal density is 25 l^{-1}, then $B(\pi)_{\parallel}$ changes from 10 to 1.5 km^{-1}, which is in rough agreement with Fig. 5 when attenuation by the lower layer is included. The corresponding number of aligned crystals in each pulse volume for $B(\pi)_{\parallel} = 10$ km^{-1} ($f = 0.16$, $\delta\xi = 2.0$, $\eta_0 = 25$ l^{-1}) is about 0.22. However, in the lidar experiment the height intervals were integrated over 100 ns, so that the average number n in ~ 15 m is predicted to be 1.1. The signal-to-noise ratio of fluctuations in the cloud profile would be $\sim n^{\frac{1}{2}} \approx 1$. Fluctuations with range do occur in the values of $B(\pi)_{\parallel}$ in Fig. 6 and these are also evident in earlier profiles (Platt, 1977), but they would indicate a signal-to-noise ratio of about 3, or 9 crystals per 15 meters. An unknown in the calculation of n is whether the crystal population is composed of fully "perfect" and "imperfect" crystals as implied in Table 1, or whether each crystal is "perfect" with a proportion $(1-f)$ of imperfect area. In the latter case, f is effectively unity in Table 1, and for the above example, the number of particles in each volume will be ~ 5 per 15 meters.

The above discussion shows qualitative agreement between Fig. 6 and theory, but the angle $\delta\xi$ was not known so it is hard to carry the comparison any further. This angle could be measured by scanning the lidar away from the vertical and noting any dramatic decrease in backscatter.

7. Conclusions

The calculations in this article have shown that large backscatter is possible from horizontally oriented ice crystals using a vertical pointing lidar. They also give the important result that the depolarization ratio from an *ice* cloud may be only a few percent. Thus low depolarization ratios from middle level clouds must be treated with caution.

Values of $B(\pi)_{\parallel}$ and Δ measured in an altostratus cloud layer agree qualitatively with a simple model in which the crystal population is composed of a fraction f of perfect crystal faces and a fraction $(1-f)$ of imperfect faces. It has also been shown that only a few crystals in each laser pulse volume are needed to give a large signal at a receiver. Calculations using realistic crystal numbers measured in actual clouds indicate that the signal could fluctuate considerably from one pulse volume to the next, even for a homogeneous cloud. Such fluctuations were observed in the altostratus cloud.

Given a reasonably horizontal homogeneous cloud layer, information on the nature of the crystal population, the presence of horizontal ice crystals and their maximum flutter could be obtained by scanning a lidar away from the vertical. Information could then be obtained on crystal numbers and even size, although the latter would be complicated by the predicted interference effect. Also, determination of the crystal number would require direct sampling of crystals to determine

the degree of riming, dendritic growth and shattering. Finally, it should be pointed out that if crystals are falling with their long axes very close to the horizontal then a lidar must be aligned very accurately in the vertical before reflections from crystal surfaces will be observed.

Acknowledgments. This work was done while the author was a Visiting Fellow at the Cooperative Institute for Research in Environmental Sciences (CIRES), University of Colorado/NOAA, Boulder, Colorado.

REFERENCES

Deirmendjian, D., 1964: Scattering and polarization properties of water clouds and hazes in the visible and infrared. *Appl. Opt.*, **3**, 187–196.

Derr, V. E., N. L. Abshire, R. E. Cupp and G. T. McNice, 1976: Depolarization of lidar returns from virga and source cloud. *J. Appl. Meteor.*, **15**, 1200–1203.

Fletcher, N. H., 1962: *The Physics of Rain Clouds*. Cambridge University Press, 86 pp.

Heymsfield, A. J., 1977: Precipitation development in stratiform ice clouds: a microphysical and dynamical study. *J. Atmos. Sci.*, **34**, 367–381.

Jayaweera, K.O.L.F., and B. J. Mason, 1965: The behavior of freely falling cylinders and cones in a viscous fluid. *J. Fluid Mech.*, **22**, 709–720.

—— and ——, 1966: The falling motions of loaded cylinders and discs simulating snow crystals. *Quart. J. Roy. Meteor. Soc.*, **92**, 151–156.

Liou, Kuo-nan, and H. Lahore, 1974: Laser sensing of cloud composition. A backscattered depolarization technique. *J. Appl. Meteor.*, **13**, 257–263.

Mason, B. J., 1971: *The Physics of Clouds*. Clarendon Press, 671 pp.

Mossop, S. C., 1968: Comparisons between concentrations of ice crystals in clouds and the concentrations of ice nuclei. *J. Rech. Atmos.*, **3**, 119–124.

Ono, A., 1969: The shape and riming properties of ice crystals in natural clouds. *J. Atmos. Sci.*, **26**, 138–147.

Platt, C. M. R., 1973: Lidar and radiometric observations of cirrus clouds. *J. Atmos. Sci.*, **30**, 1191–1204.

——, 1977: Lidar observations of a mixed-phase altostratus cloud. *J. Appl. Meteor.*, **16**, 339–345.

Sassen, K., 1974: Depolarization of laser light backscattered by artificial ice clouds. *J. Appl. Meteor.*, **13**, 923–933.

——, 1977: Ice crystal habit discrimination with the optical backscatter depolarization technique. *J. Appl. Meteor.*, **16**, 425–431.

Schotland, R. M., K. Sassen and R. Stone, 1971: Observations by lidar of linear depolarization ratios for hydrometeors. *J. Appl. Meteor.*, **10**, 1011–1017.